Adaptive Control of KNTU Planar Cable-Driven Parallel Robot with Uncertainties in Dynamic and Kinematic Parameters

Reza Babaghasabha, Mohammad A. Khosravi and Hamid D. Taghirad

Abstract This paper addresses the design and implementation of adaptive control on a planar cable-driven parallel robot with uncertainties in dynamic and kinematic parameters. To develop the idea, firstly, adaptation is performed on dynamic parameters and it is shown that the controller is stable despite the kinematic uncertainties. Then, internal force term is linearly separated into a regressor matrix in addition to a kinematic parameter vector that contains estimation error. In the next step to improve the controller performance, adaptation is performed on both the dynamic and kinematic parameters. It is shown that the performance of the proposed controller is improved by correction in the internal forces. The proposed controller not only keeps all cables in tension for the whole workspace of the robot, it is computationally simple and it does not require measurement of the end-effector acceleration as well. Finally, the effectiveness of the proposed control algorithm is examined through some experiments on KNTU planar cable-driven parallel robot and it is shown that the proposed control algorithm is able to provide suitable performance in practice.

1 Introduction

Cable-driven parallel robots have some positive features such as large workspace [1, 2], high speed manipulation [3], high payload to robot weight ratio [4], transportability and ease of assembly/disassembly. Despite all advantages listed for this class of robots, using cables in the robot structure introduces new challenges in the study of cable-driven parallel robots. Cables are able to apply only tensile forces, and in order to avoid structural failures, design of control algorithms should be performed

R. Babaghasabha (✉) · M.A. Khosravi (✉) · H.D. Taghirad (✉)
Advanced Robotics and Automated Systems (ARAS), Faculty of Electrical Engineering, Industrial Control Center of Excellence (ICCE), K. N. Toosi University of Technology, P.O. Box 6315-1355, Tehran, Iran
e-mail: Reza.bgha@mail.kntu.ac.ir

M.A. Khosravi
e-mail: Makh@ee.kntu.ac.ir

H.D. Taghirad
e-mail: Taghirad@kntu.ac.ir

A. Pott and T. Bruckmann (eds.), *Cable-Driven Parallel Robots*,
Mechanisms and Machine Science 32, DOI 10.1007/978-3-319-09489-2_11

such that the cables remain in tension for the whole workspace of the robot. These features make feedback control of the cable-driven parallel robots more challenging than that of the conventional parallel robots.

Motion control topologies of the cable-driven parallel robots may be classified into two categories, the ones that are formed in the cable length coordinates and the others that are designed in the task space coordinates. In [3, 5] decentralized controllers have been proposed in the cable length coordinates and their performance has been evaluated through some experiments. In this framework the length of the cables can be simply measured by the encoders. Therefore, the controllers can be implemented economically in practice. However, in applications with high accuracy and high bandwidth, using the cable lengths measurement in the control algorithms is not reliable due to the inherent flexibility of the cables. Moreover, the main control aim is to realize the trajectory tracking in the task space. Therefore, suitable control accuracy can be achieved only when the task space tracking error is used as the feedback to the controller without any kinematic transformation.

In task space control topologies, the pose of the end-effector shall be measured directly. This measurement requires high-tech and expensive instrumentation system such as laser ranging equipment or inertial measurement unit. For this reason, only few researches focus on implementation of the task space controllers in practice. In [6] laser ranging equipment has been used to measure the end-effector pose of the 6-DOF cable-driven parallel robot in the task space coordinates. In [7] the PID controller is designed and implemented in the task space coordinates. However, in order to avoid direct pose measurement, length of the cables is measured by the encoders and the pose of the end-effector is estimated by forward kinematic analysis. As mentioned earlier, using cable length information is not reliable due to the inherent flexibility of the cables. In addition, solving the forward kinematics equations of the robot in the feedback loop reduces the measurement accuracy and limits the controller bandwidth due to the complexity and multiplicity of the solutions. Computer vision is another way for direct measurement of the end-effector pose and it can be used as a suitable and economical alternative. In [8] Vision-based pose measurement is performed on a planar cable-driven parallel robot. But only the translational motion is measured and the end-effector rotation is not considered.

Classic controllers such as PID [7] have simple structures and do not require complete dynamic model of the cable-driven parallel robot. However, due to the lack of consideration of dynamic effects in the structure of the controller, it may only operate suitably in regulation problems, while have limited performance in tracking objectives. On the other hand, internal forces which are used in the controller to ensure that all cables remain in tension, shall span the null space of the Jacobian matrix appropriately. However, uncertainties in kinematic parameters affect on the internal forces and degrade performance of the controller even in regulation problems.

Inclusion of the dynamic behavior of the robot in design of nonlinear controllers [9–12] can improve the performance of the controller in tracking purposes. However, detailed information of the dynamic and kinematic models of the robot is required to implement this controllers. Furthermore, it shall be noted that precise knowledge on kinematics and dynamics of the robot is unavailable in practice, and this may

significantly limit the tracking performance. To partially remedy this shortcoming, calibration methods may be applied to identify near true parameters. However, robot calibration process is time consuming and requires expensive and precise measurement units. These all shortcomings may be remedied by using an adaptive controller in task space coordinates in which the kinematic and dynamic parameters are simultaneously adapted.

As a representative of such method, in [8] robust PD controller with an adaptive compensation term has been used. It has been shown that measuring both the cables length and the pose of the end-effector in real-time enables the designer to linearly separate the internal force term into a regressor matrix and a kinematic parameter vector. In this paper the performance of the controller has been evaluated only in regulation problem through some experiments on a translational system using the minimum number of cables under zero-gravity condition. In addition, the dynamic model of the robot has not been used in the controller structure and consequently, the adaptation has not been performed on dynamic parameters. Furthermore, a large number of kinematic parameters have been adapted and therefore, updating the kinematic parameters becomes difficult.

In this paper, an adaptive controller is designed in task space coordinates for a planar cable-driven parallel robot with uncertainties in dynamic and kinematic parameters. In the first section of controller design, adaptation is performed only on dynamic parameters and it is shown that the controller is stable despite kinematic uncertainties. Next, real-time measurement of the cable length through encoders and that of the pose of the end-effector through a CCD camera is used to linearly separate the internal force term into a regressor matrix and a kinematic parameter vector that contains estimation error. In this paper, vision-based pose measurement is chosen as a suitable and economical solution. Then, adaptation is performed on both the dynamic and kinematic parameters and it is shown that the performance of the proposed controller is significantly improved by the correction of the internal forces. In addition, the proposed controller is able to keep all the cables in tension for the whole workspace of the robot. Finally, to show the effectiveness of proposed control algorithm some experiments are performed on KNTU planar cable-driven parallel robot and it is shown that the proposed control algorithm is able to provide suitable performance in practice.

2 Robot Dynamics and Kinematics

The dynamic model of a planar cable-driven parallel robot without considering the flexibility of the cables can be written as [13]

$$\mathbf{M}(\mathbf{x})\ddot{\mathbf{x}} + \mathbf{C}(\mathbf{x},\dot{\mathbf{x}})\dot{\mathbf{x}} + \mathbf{G}(\mathbf{x}) = \mathbf{f} = -\mathbf{J}^T\tau \tag{1}$$

in which, $\mathbf{x}$ denotes the generalized coordinates vector for pose of the end-effector, τ denotes the vector of cable forces and $\mathbf{f}$ is the vector of Cartesian wrench. $\mathbf{M}(\mathbf{x})$ denotes mass matrix of the robot, $\mathbf{C}(\mathbf{x},\dot{\mathbf{x}})$ denotes Coriolis and centrifugal terms,

$\mathbf{G}(\mathbf{x})$ denotes the vector of gravity terms and $\mathbf{J}$ denotes the Jacobian matrix of the robot. Some important properties of the dynamic equation described by (1) are listed as follows [13].

Property 1: The mass matrix $\mathbf{M}(\mathbf{x})$ is symmetric and uniformly positive definite for all $\mathbf{x}$.

Property 2: The matrix $\dot{\mathbf{M}}(\mathbf{x}) - \mathbf{2C}(\mathbf{x},\dot{\mathbf{x}})$ is skew-symmetric, and therefore the expression $\mathbf{Z}^T(\dot{\mathbf{M}}(\mathbf{x}) - \mathbf{2C}(\mathbf{x},\dot{\mathbf{x}}))Z$ is equal to zero, for all $\mathbf{Z}$.

Property 3: The dynamic model described by (1) may be represented by a linear regressor with respect to a set of dynamic parameters as

$$\mathbf{M}(\mathbf{x})\ddot{\mathbf{x}} + \mathbf{C}(\mathbf{x},\dot{\mathbf{x}})\dot{\mathbf{x}} + \mathbf{G}(\mathbf{x}) = \mathbf{Y}_D(\mathbf{x},\dot{\mathbf{x}},\ddot{\mathbf{x}})\mathbf{a} \tag{2}$$

where $\mathbf{Y}_D(\mathbf{x},\dot{\mathbf{x}},\ddot{\mathbf{x}})$ denotes the regressor matrix and $\mathbf{a}$ denotes dynamic parameters vector. In [13] kinematic and dynamic analysis for a planar cable-driven parallel robot have been reported in detail and it is shown that the dynamic model as described by (1) can be written into the linear regression form. KNTU planar cable-driven parallel robot consists of an end-effector that is connected by four cables to the base platform as shown in Fig. 1. Using massless rigid string model for the cable, the equations of motion for this robot may be written as follows:

$$\mathbf{M}(\mathbf{x})\ddot{\mathbf{x}} + \mathbf{G}(\mathbf{x}) = \mathbf{f} = -\mathbf{J}^T\tau \tag{3}$$

in which,

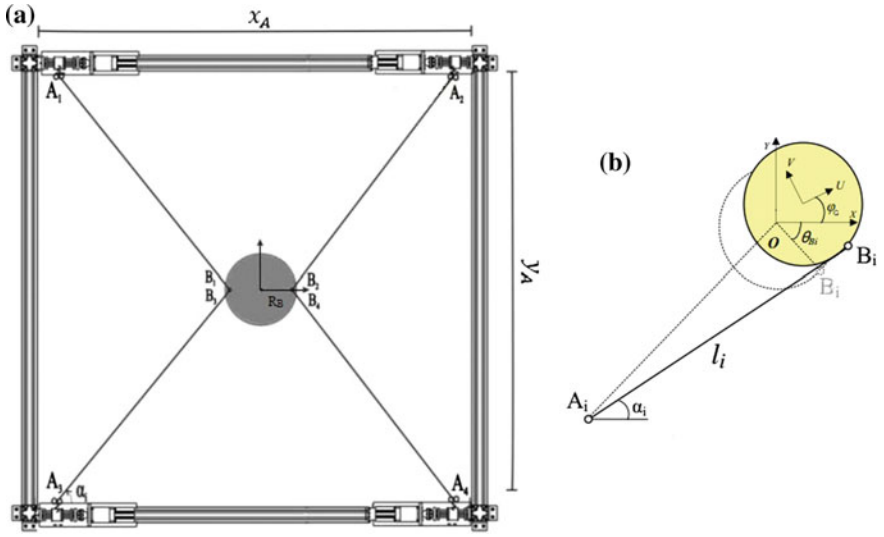

Fig. 1 **a** The schematics of KNTU cable-driven robot. **b** Kinematic configuration of mechanism

$$\mathbf{M} = \begin{bmatrix} m & 0 & 0 \\ 0 & m & 0 \\ 0 & 0 & I_z \end{bmatrix} \quad \mathbf{G} = \begin{bmatrix} 0 \\ mg \\ 0 \end{bmatrix}$$

where m is the mass and I_z is the moment of inertia of the end-effector about its center of mass and g is the gravity acceleration. The Jacobian matrix of the robot can be expressed by

$$\mathbf{J}^T = \begin{bmatrix} S_{1x} & S_{2x} & S_{3x} & S_{4x} \\ S_{1y} & S_{2y} & S_{3y} & S_{4y} \\ S_{1z} & S_{2z} & S_{3z} & S_{4z} \end{bmatrix} \tag{4}$$

in which,

$$S_{ix} = \frac{x_G - 0.5x_A + R_B \cos(\phi_i)}{l_i}$$
$$S_{iy} = \frac{y_G - 0.5y_A + R_B \sin(\phi_i)}{l_i}$$
$$S_{iz} = R_B \cos(\phi_i) S_{iy} - R_B \sin(\phi_i) S_{ix}$$

and $\mathbf{x} = [x_G, y_G, \phi_G]$ denotes the generalized coordinate vector for the pose of the end-effector, x_A and y_A are the length and width of the rectangle that actuators have been attached on its vertices, l_i is the cables length, B_i is the attachment point of the cables on the end-effector which lies at the radial distance of R_B from center of the end-effector, $\phi_i = \phi_G + \theta_{B_i}$ is instantaneous orientation angle of the moving attachment point and θ_{B_i} is its absolute angular position, respectively.

3 Controller Design

3.1 Adaptation of Dynamic Parameters

In this section, an adaptive controller is proposed for the planar cable-driven parallel robots with uncertainties in dynamic and kinematic parameters. To derive the control and adaptation laws, consider the following Lyapunov function candidate as [14]

$$V(t) = \frac{1}{2}(\mathbf{S}^T \mathbf{M} \mathbf{S} + \tilde{\mathbf{a}}^T \Gamma_D \tilde{\mathbf{a}}) \tag{5}$$

in which,

$$\mathbf{S} = \dot{\tilde{\mathbf{x}}} + \Lambda \tilde{\mathbf{x}}$$

where $\mathbf{S}$ denotes a sliding surface, Γ_D and Λ are symmetric diagonal positive definite matrices, $\tilde{\mathbf{x}} = \mathbf{x} - \mathbf{x}_d$ is the tracking error vector and $\tilde{\mathbf{a}} = \hat{\mathbf{a}} - \mathbf{a}$ denotes the dynamic parameter estimation error vector. Differentiate $V(t)$ with respect to time:

$$\dot{V}(t) = \mathbf{S}^T \mathbf{M}\dot{\mathbf{S}} + \frac{1}{2}\mathbf{S}^T \dot{\mathbf{M}}\mathbf{S} + \tilde{\mathbf{a}}^T \Gamma_D \dot{\tilde{\mathbf{a}}} \tag{6}$$

$$\dot{V}(t) = \mathbf{S}^T \mathbf{M}(\ddot{\tilde{\mathbf{x}}} + \Lambda\dot{\tilde{\mathbf{x}}}) + \mathbf{S}^T [\frac{1}{2}(\dot{\mathbf{M}} - \mathbf{2C}) + \mathbf{C}]\mathbf{S} + \tilde{\mathbf{a}}^T \Gamma_D \dot{\tilde{\mathbf{a}}} \tag{7}$$

Using skew-symmetricity of $\dot{\mathbf{M}} - \mathbf{2C}$ and substitution from (1) yields

$$\dot{V}(t) = \mathbf{S}^T (-\mathbf{J}^T \tau - \mathbf{C}\dot{\mathbf{x}} - \mathbf{G} - \mathbf{M}\ddot{\mathbf{x}}_d + \mathbf{M}\Lambda\dot{\tilde{\mathbf{x}}} + \mathbf{CS}) + \tilde{\mathbf{a}}^T \Gamma_D \dot{\tilde{\mathbf{a}}} \tag{8}$$

Define the virtual reference trajectory as

$$\mathbf{x}_r = \mathbf{x}_d - \Lambda \int_0^t \tilde{\mathbf{x}} dt \tag{9}$$

Differentiate $\mathbf{x}_r$ twice with respect to time, and substitute into Eq. (8):

$$\dot{V}(t) = \mathbf{S}^T (-\mathbf{J}^T \tau - \mathbf{M}\ddot{\mathbf{x}}_r - \mathbf{C}\dot{\mathbf{x}}_r - \mathbf{G}) + \tilde{\mathbf{a}}^T \Gamma_D \dot{\tilde{\mathbf{a}}} \tag{10}$$

For the purpose of stability of the closed loop system, let us define the control law as

$$\mathbf{f} = -\hat{\mathbf{J}}^T \tau = \hat{\mathbf{M}}\ddot{\mathbf{x}}_r + \hat{\mathbf{C}}\dot{\mathbf{x}}_r + \hat{\mathbf{G}} - \mathbf{K}_D \mathbf{S} \tag{11}$$

where $\mathbf{K}_D$ denotes symmetric diagonal positive definite matrix and $\hat{\mathbf{J}}^T$ denotes uncertain Jacobian matrix of the robot. In practice the attachment points are not precisely implemented in practice. Therefore, it is assumed to have an uncertain Jacobian matrix obtained from uncertain kinematic parameters. The general solution of (11) for τ is

$$\tau = \overline{\tau} + \mathbf{Q} \tag{12}$$

where $\overline{\tau}$ is the minimum solution of (11) and derived by using the pseudo-inverse of $\hat{\mathbf{J}}^T$ and is given by

$$\overline{\boldsymbol{\tau}} = -\hat{\mathbf{J}}(\hat{\mathbf{J}}^T \hat{\mathbf{J}})^{-1} = -\hat{\mathbf{J}}^{\dagger}\mathbf{f} \tag{13}$$

and $\mathbf{Q}$ may be physically interpreted as the internal forces that spans the null space of $\hat{\mathbf{J}}^T$. Therefore,

$$\hat{\mathbf{J}}^T \mathbf{Q} = 0 \tag{14}$$

Internal forces are used to ensure that all cables remain in tension within the whole workspace. Moreover, term can be used to increase the robot stiffness [15]. Now, substitute the control law (11) into Eq. (10). This yields to:

$$\begin{aligned}\dot{V}(t) &= \mathbf{S}^T[(\mathbf{J}^T\hat{\mathbf{J}}^{\dagger})\mathbf{f} - \mathbf{J}^T\mathbf{Q} - \mathbf{M}\ddot{\mathbf{x}}_r - \mathbf{C}\dot{\mathbf{x}}_r - \mathbf{G})] + \tilde{\mathbf{a}}^T\Gamma_D\dot{\tilde{\mathbf{a}}} \\ &= \mathbf{S}^T[(\mathbf{J}^T\hat{\mathbf{J}}^{\dagger})\mathbf{f} + \mathbf{f} - \mathbf{f} - \mathbf{J}^T\mathbf{Q} + \hat{\mathbf{J}}^T\mathbf{Q} - \mathbf{M}\ddot{\mathbf{x}}_r - \mathbf{C}\dot{\mathbf{x}}_r - \mathbf{G})] + \tilde{\mathbf{a}}^T\Gamma_D\dot{\tilde{\mathbf{a}}} \\ &= \mathbf{S}^T[\tilde{\mathbf{M}}\ddot{\mathbf{x}}_r + \tilde{\mathbf{C}}\dot{\mathbf{x}}_r + \tilde{\mathbf{G}} - \mathbf{K}_D\mathbf{S} + (\hat{\mathbf{J}}^T - \mathbf{J}^T)\mathbf{Q} - (\mathbf{I} - \mathbf{J}^T\hat{\mathbf{J}}^{\dagger})\mathbf{f}] + \tilde{\mathbf{a}}^T\Gamma_D\dot{\tilde{\mathbf{a}}}\end{aligned} \tag{15}$$

in which

$$\tilde{\mathbf{M}} = \hat{\mathbf{M}} - \mathbf{M}, \quad \tilde{\mathbf{C}} = \hat{\mathbf{C}} - \mathbf{C}, \quad \tilde{\mathbf{G}} = \hat{\mathbf{G}} - \mathbf{G}$$

Since the matrices **M**,**C** and **G** are linear in terms of the manipulator parameters, we may separate the dynamic model of a planar cable-driven parallel robot into a linear regressor matrix and a vector of parameters as

$$\tilde{\mathbf{M}}\ddot{\mathbf{x}}_r + \tilde{\mathbf{C}}\dot{\mathbf{x}}_r + \tilde{\mathbf{G}} = \mathbf{Y}_D(\mathbf{x}, \dot{\mathbf{x}}, \dot{\mathbf{x}}_r, \ddot{\mathbf{x}}_r)\tilde{\mathbf{a}} \tag{16}$$

Substitution above equation into Eq. (15) yields to

$$\dot{V}(t) = \mathbf{S}^T[\mathbf{Y}_D(\mathbf{x}, \dot{\mathbf{x}}, \dot{\mathbf{x}}_r, \ddot{\mathbf{x}}_r)\tilde{\mathbf{a}} - \mathbf{K}_D\mathbf{S} + (\hat{\mathbf{J}}^T - \mathbf{J}^T)\mathbf{Q} - (\mathbf{I} - \mathbf{J}^T\hat{\mathbf{J}}^{\dagger})\mathbf{f}] + \tilde{\mathbf{a}}^T\Gamma_D\dot{\tilde{\mathbf{a}}}. \tag{17}$$

Let us define the dynamic adaptation law as

$$\dot{\tilde{\mathbf{a}}} = -\Gamma_D^{-1}\mathbf{Y}_D^T(\mathbf{x}, \dot{\mathbf{x}}, \dot{\mathbf{x}}_r, \ddot{\mathbf{x}}_r)\mathbf{S} \tag{18}$$

By using the above adaptation law the resulting expression of $\dot{V}(t)$ is reduced to

$$\dot{V}(t) = \mathbf{S}^T[-\mathbf{K}_D\mathbf{S} + (\hat{\mathbf{J}}^T - \mathbf{J}^T)\mathbf{Q} - (\mathbf{I} - \mathbf{J}^T\hat{\mathbf{J}}^{\dagger})\mathbf{f}] \tag{19}$$

The uncertain jacobian matrix $\hat{\mathbf{J}}^T$, and the internal forces may be assumed to be bounded by the following relations:

$$\|\hat{\mathbf{J}}^T - \mathbf{J}^T\| \leq \delta_1, \quad \|\mathbf{I} - \mathbf{J}^T\hat{\mathbf{J}}^{\dagger}\| \leq \delta_2, \quad \|\mathbf{Q}\| \leq \delta_3 \tag{20}$$

Therefore, the proposed adaptive controller can certainly stabilize the closed loop system by appropriate choice of large enough $\mathbf{K}_D$. However, uncertainties in the kinematic parameters affect on the internal forces and degrade the performance of the proposed controller.

3.2 Adaptation of Kinematic Parameters

In the previous section, the stability of the proposed adaptive controller was proved despite uncertainties in kinematic parameters. However, uncertainties in kinematic parameters may change the direction of the resultant internal force and may consequently degrade the performance of the controller. Furthermore, increasing the control gains may not effective to improve the performance of the controller and it causes greater impact of the internal forces which do not appropriately span the null space of the Jacobian matrix. In order to overcome this shortcoming, the important internal force term may be also separated into a linear regressor matrix and a kinematic parameter vector expressed by

$$(\hat{\mathbf{J}}^T - \mathbf{J}^T)\mathbf{Q} = \tilde{\mathbf{J}}^T\mathbf{Q} = \mathbf{Y}_K(\mathbf{x}, \mathbf{L}, \mathbf{Q})\tilde{\mathbf{b}} \tag{21}$$

where $\mathbf{Y}_K(\mathbf{x}, \mathbf{L}, \mathbf{Q})$ denotes the regressor matrix, and for a planar cable-driven parallel robot with four actuated cable driven limbs, $\mathbf{L} = [l_1, l_2, l_3, l_4]$ denotes the cables length, $\mathbf{Q} = [q_1, q_2, q_3, q_4]$ denotes the internal force vector and $\tilde{\mathbf{b}} = \hat{\mathbf{b}} - \mathbf{b}$ denotes the kinematic parameters estimation error vector. According to kinematic equation of KNTU planar cable-driven parallel robot and by some manipulations, Eq. (21) may be derived in an explicit form as

$$\mathbf{Y}_K(\mathbf{x}, \mathbf{L}, \mathbf{Q})\tilde{\mathbf{b}} = \begin{bmatrix} Y_{11} & 0 & Y_{13} & 0 & 0 \\ 0 & Y_{22} & Y_{23} & 0 & 0 \\ 0 & 0 & Y_{33} & Y_{34} & Y_{35} \end{bmatrix} \begin{bmatrix} x_A \\ y_A \\ R_B \\ x_A R_B \\ y_A R_B \end{bmatrix} \tag{22}$$

in which,

$$Y_{11} = \frac{1}{2}\left(\frac{q_1}{l_1} - \frac{q_2}{l_2} + \frac{q_3}{l_3} - \frac{q_4}{l_4}\right), \quad Y_{13} = \sum_{i=1}^{4} \frac{q_i \cos(\phi_i)}{l_i},$$

$$Y_{22} = \frac{1}{2}\left(-\frac{q_1}{l_1} - \frac{q_2}{l_2} + \frac{q_3}{l_3} + \frac{q_4}{l_4}\right), \quad Y_{23} = \sum_{i=1}^{4} \frac{q_i \sin(\phi_i)}{l_i},$$

$$Y_{33} = \sum_{i=1}^{4} \frac{q_i}{l_i}(y_G \cos(\phi_i) - x_G \sin(\phi_i)), \quad Y_{34} = \frac{1}{2}\sum_{i=1}^{4}(-1)^i\left[\frac{q_i \sin(\phi_i)}{l_i}\right],$$

$$Y_{35} = \frac{1}{2}\left(-\frac{q_1 \cos(\phi_1)}{l_1} - \frac{q_2 \cos(\phi_2)}{l_2} + \frac{q_3 \cos(\phi_3)}{l_3} + \frac{q_4 \cos(\phi_4)}{l_4}\right).$$

Now, one can propose a new Lyapunov function candidate as following:

$$V(t) = \frac{1}{2}(\mathbf{S}^T\mathbf{M}\mathbf{S} + \tilde{\mathbf{a}}^T\Gamma_D\tilde{\mathbf{a}} + \tilde{\mathbf{b}}^T\Gamma_K\tilde{\mathbf{b}}) \tag{23}$$

in which, Γ_K is a symmetric positive definite matrix. Differentiate $V(t)$ with respect to time, and according to the formulations given in previous section, substitute the control law and the dynamic adaptation law into Eq. (23). By some manipulation and using Eq. (21), one may obtain the following relation.

$$\dot{V}(t) = \mathbf{S}^T[-\mathbf{K}_D\mathbf{S} + \mathbf{Y}_K(\mathbf{x}, \mathbf{L}, \mathbf{Q})\tilde{\mathbf{b}} - (\mathbf{I} - \mathbf{J}^T\hat{\mathbf{J}}^\dagger)\mathbf{f}] + \tilde{\mathbf{b}}^T\Gamma_K\dot{\tilde{\mathbf{b}}} \tag{24}$$

By considering the kinematic adaptation law as

$$\dot{\hat{\mathbf{b}}} = -\Gamma_K^{-1}\mathbf{Y}_K^T(\mathbf{x}, \mathbf{L}, \mathbf{Q})\mathbf{S} \tag{25}$$

the resulting expression of $\dot{V}(t)$ yields to

$$\dot{V}(t) = \mathbf{S}^T[-\mathbf{K}_D\mathbf{S} - (\mathbf{I} - \mathbf{J}^T\hat{\mathbf{J}}^\dagger)\mathbf{f}] \tag{26}$$

Expression (26) is negative semi-definite by choosing $\mathbf{K}_D$ large enough and it shows that the proposed adaptive controller can stabilize the system. Moreover, adaptation of kinematic parameters with adaptation law in Eq. (25) will significantly improve the performance of the proposed controller by adjusting the direction of the resultant internal forces. If the estimation error of the kinematic parameters is zero, the resulting expression of $\dot{V}(t)$ yields to

$$\dot{V}(t) = -\mathbf{S}^T\mathbf{K}_D\mathbf{S} \leq 0 \tag{27}$$

Therefore, the trajectories of the closed loop system will eventually converges to the sliding surface,

$$\mathbf{S} = \dot{\tilde{\mathbf{x}}} + \Lambda\tilde{\mathbf{x}} = 0 \tag{28}$$

and therefore, the proposed adaptive controller guarantees zero steady-state tracking error for the pose of the end-effector. But it is notable that the dynamic and kinematic parameters can not necessarily converge to their exact values. This means that the tracking error will remain uniformly ultimately bounded (UUB) by choosing $\mathbf{K}_D$ large enough.

4 Experimental Results

In order to verify the effectiveness of the proposed adaptive controller, it is applied to KNTU planar cable-driven parallel robot. This manipulator is under investigation for high speed and wide workspace applications in Advanced Robotics and Automated Systems (ARAS) group of K. N. Toosi University of Technology (KNTU).

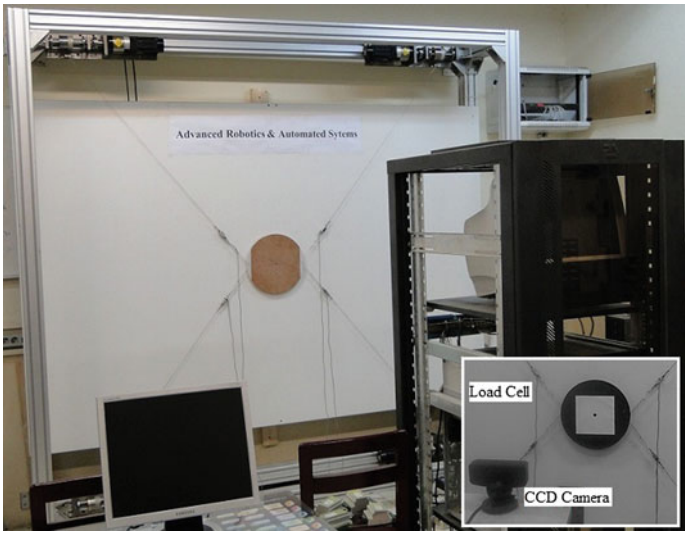

Fig. 2 KNTU planar cable-driven parallel robot

4.1 KNTU Planar Cable-Driven Parallel Robot

KNTU planar cable-driven parallel robot consists of four actuated cable driven limbs with three degrees of freedom planar motion which is shown in Fig. 2. Actuators are located on the vertices of a rectangle with dimension of $2.24 \times 2.1\,\mathrm{m}$ and the radial distance of attachment points of the cables from center of the end-effector is considered as $R_B = 15\,\mathrm{cm}$. Moreover, mass and moment of inertia of the end-effector is considered as $m = 5\,\mathrm{kg}$ and $I_z = 0.1\,\mathrm{kg\,m^2}$, respectively. All of the dynamic and kinematic parameters mentioned above, considered to be uncertain. In addition, a CCD camera with resolution of 320×240 pixels and frame rate of 100 fps at the distance of 1.12 m from the plane of motion of the end effector is used to directly measure the pose of the end-effector. In order to determine the pose of the end effector, at least four coplanar non-aligned features on the object are required [16]. For this reason, a square marker is used for fast and accurate tracking and the pose of the end-effector is measured by extracting corners using Harris corner detector [17] in real-time. The resolution of the measurement of the position and orientation of the end-effector are 0.1 mm and 0.2°, respectively. Furthermore, The sampling time of the control loop is one millisecond which provides real time execution of the proposed controller.

4.2 Control Scheme

To have a desirable performance in position and orientation tracking, it is necessary to have ideal torque sources as the actuators. In practice, however, the actuator drivers

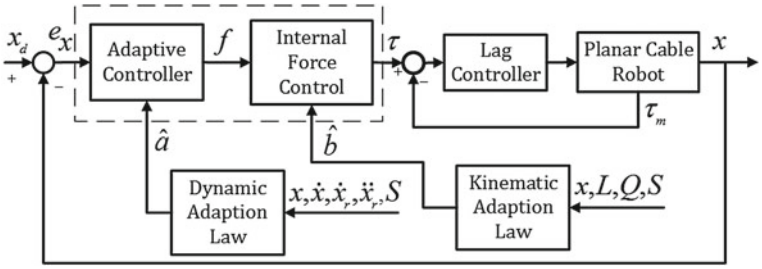

Fig. 3 Block diagram of proposed adaptive controller

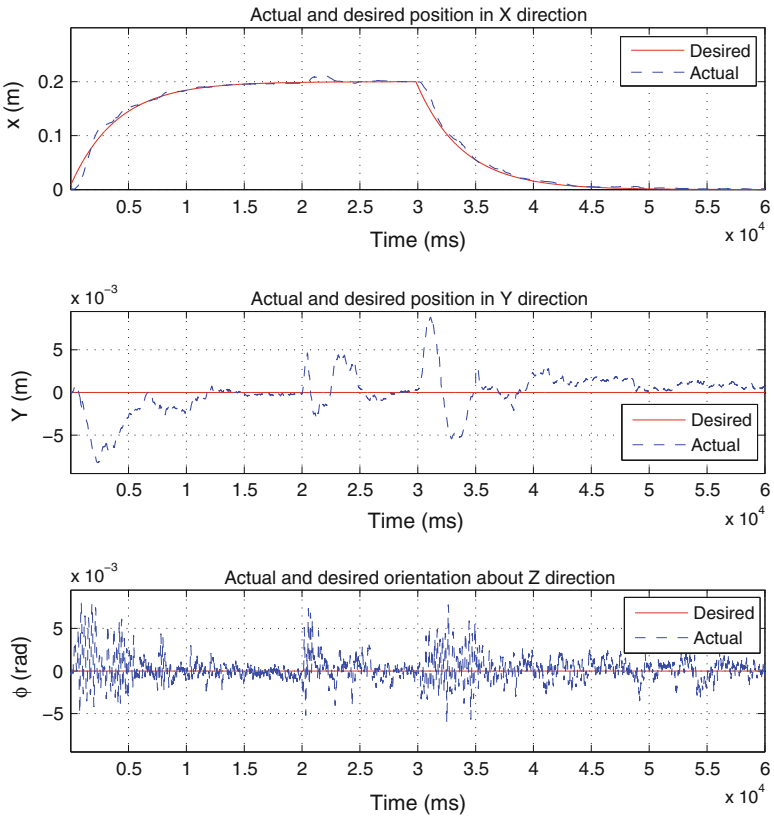

Fig. 4 Actual and desired position and orientation of the end-effector in the first experiment

suffer from a number of limitations, and cannot perform as ideal torque sources. In order to overcome this shortcoming, cascade control scheme is implemented in the experiments. The cascade control strategy uses two control loops, called outer and inner loops as shown in Fig. 3. In the proposed control algorithm, while adaptive

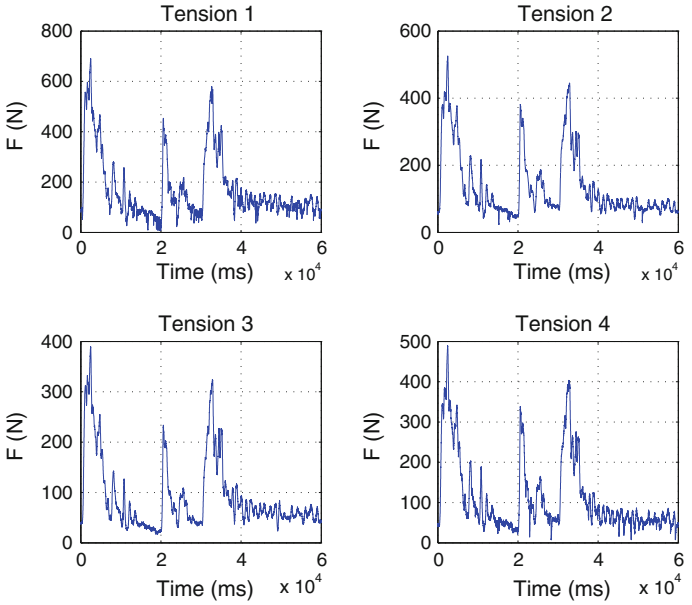

Fig. 5 Cables tension in the first experiment

controller controls the pose of the end-effector in the outer loop, a lag controller is designed in the inner loop to regulate the cables tension, and prevents them from tearing. Inputs of adaptive controller are position and orientation errors and dynamic parameter estimation vector, while its outputs are the required Cartesian wrench. The calculated output wrench is transformed into positive actuator forces through the internal force control block. This block uses kinematic parameter estimation vector to find the internal forces that span appropriately the null space of the Jacobian matrix. Next, the resulting desired positive tensions are compared to the actual tensions measured by the load cells located near the end-effector attachment points. TLL500 from Transducer Techniques is used to measure the cable tensions in the setup. The proposed controller is implemented using RT-LAB software [18] and the equations of internal forces are solved by CFSQP implemented as an s-function in Simulink.

4.3 Results

In order to verify the effectiveness of the proposed adaptive controller, two disjointed motions in translation and rotation are considered. In the first experiment, the following exponential trajectory is considered in x direction, while the end-effector attempts to maintain $y = 0$ and $\phi = 0$ during the motion.

$$x_d = \begin{cases} 0.2(1 - e^{-0.25t}) & t < 30 \\ 0.2e^{-0.25(t-30)} & t \geq 30 \end{cases}$$

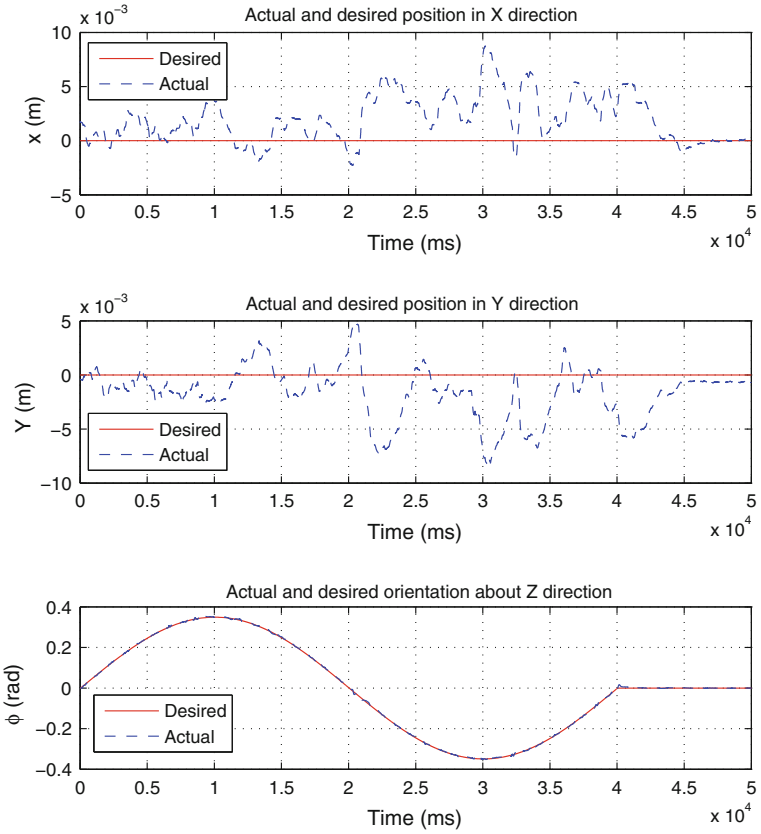

Fig. 6 Actual and desired position and orientation of the end-effector in the second experiment

The results of implementation using the proposed controller in tracking desired trajectories are given in Figs. 4, 5. Figure 4 illustrates the tracking errors in three directions, while Fig. 5 provides the cable forces measured by the load cells located near the end-effector attachment points. The controller gain is selected such that the stability of the controller is guaranteed, as $K_D = 1200$. As it is seen in Fig. 4 the pose of the end-effector can suitably track the desired trajectories and the errors are very small and in order of 10^{-3}. Moreover, as it is shown in Fig. 5 all cables remain in tension during the robot maneuvers. In the second experiment, the following sinusoidal trajectory is considered in ϕ direction, and it is considered that the end-effector has no motion in the other directions.

$$\phi_d = \begin{cases} \frac{\pi}{9} \sin\left(\frac{\pi}{20} t\right) & t < 40 \\ 0 & t \geq 40 \end{cases}$$

The tracking errors in three directions is shown in Fig. 6, while Fig. 7 provides the cables tension. As it is seen in Fig. 6 the proposed controller provide the suitable per-

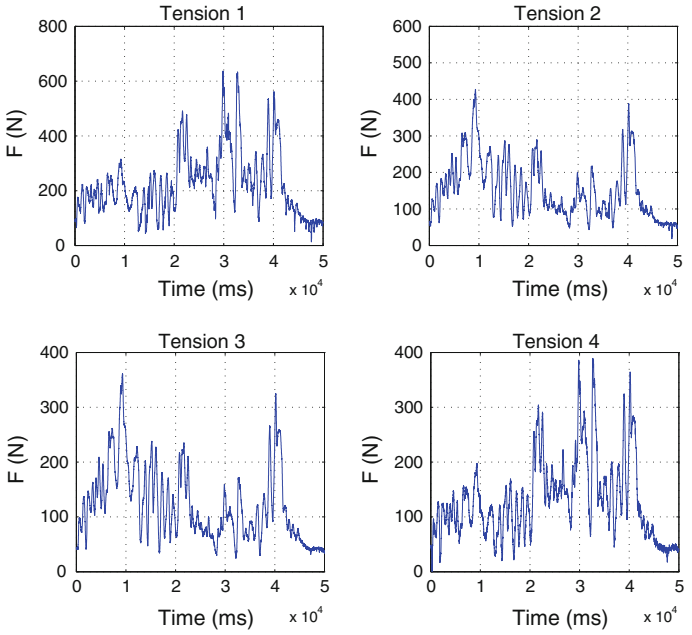

Fig. 7 Cables tension in the second experiment

formance in tracking and the errors are very small and in order of 10^{-3}. Furthermore, Fig. 7 shows that all cables remain in tension during the robot movements.

Small errors in tracking the desired trajectories are observed in this experiment. These errors may arise from the elasticity of the cables that are neglected in this analysis. The cable elasticity may lead to positioning errors, especially at high speed maneuvers. Future research is currently proceed to reduce these errors by considering elasticity of the cables in modeling and control of the robot.

5 Conclusion

In this paper, an adaptive controller is designed and implemented on a planar cable-driven parallel robot. Since some of the kinematic and dynamic parameters of the robot are uncertain, adaptation is performed on both the kinematic and dynamic parameters. It is shown that adaptation of the kinematic parameters improves the performance of the proposed controller by adjusting the direction of the resultant internal force. In addition, the controller keeps all cables in tension for the whole workspace of the robot. In order to show the effectiveness of the proposed controller, several experiments on a three degrees of freedom planar cable-driven parallel robot are performed with different desired trajectories and suitable tracking performances of some of the experiments are reported.

References

1. Taghirad HD, Nahon M (2008) Kinematic analysis of a macro-micro redundantly actuated parallel manipulator. Adv Robot 22(6–7):657–687
2. Cone LL (1985) Skycam: an aerial robotic camera system. Byte 10(10):122–132
3. Kawamura S, Kino H, Won C (2000) High-speed manipulation by using parallel wire-driven robots. Robotica 18(01):13–21
4. Albus J et al (1993) The nist robocrane. J Rob Syst 10(5):709–724
5. Fang S, Franitza D, Torlo M, Bekes F, Hiller M (2004) Motion control of a tendon-based parallel manipulator using optimal tension distribution. IEEE/ASME Trans Mechatron 9(3):561–568
6. Zi B, Duan BY, Du JL, Bao H (2008) Dynamic modeling and active control of a cable-suspended parallel robot. Mechatronics 18(1):1–12
7. Khosravi MA, Taghirad HD (2014) Robust PID control of fully-constrained cable driven parallel robots. Mechatronics 24(2):87–97
8. Kino H et al (2007) Robust pd control using adaptive compensation for completely restrained parallel-wire driven robots: translational systems using the minimum number of wires under zero-gravity condition. IEEE Trans Rob 23(4):803–812
9. Oh S-R, Agrawal SK (2005) Cable suspended planar robots with redundant cables: controllers with positive tensions. IEEE Trans Rob 21(3):457–465
10. Oh S-R, Agrawal SK (2006) Generation of feasible set points and control of a cable robot. IEEE Trans Rob 22(3):551–558
11. Oh S-R et al (2005) A dual-stage planar cable robot: dynamic modeling and design of a robust controller with positive inputs. J Mech Des 127:612
12. Williams RL, Gallina P, Vadia J (2003) Planar translational cable-direct-driven robots. J Robotic Syst 20(3):107–120
13. Taghirad HD (2013) Parallel robots: mechanics and control. CRC Press, Boca Raton
14. Slotine JJE, Li W (1987) On the adaptive control of robot manipulators. Int J Rob Res 6(3): 49–59
15. Behzadipour S, Khajepour A (2006) Stiffness of cable-based parallel manipulators with application to stability analysis. J Mech Des 128:303
16. Yuan JS-C (1989) A general photogrammetric method for determining object position and orientation. IEEE Trans Rob Autom 5(2):129–142
17. Harris C, Stephens M (1988) A combined corner and edge detector. In: Alvey vision conference, vol 15, p 50. Manchester, UK
18. Opal-RT Company (2005) Rt-lab version 8 user guide